



OPEN ACCESS

# Echocardiographic evaluation of four giant Aldabra tortoises (*Aldabrachelys gigantea*)

Marco Campolo,<sup>1</sup> Stefano Oricco,<sup>2</sup> Paolo Cavicchio,<sup>3</sup> Sara Piga,<sup>4</sup> Valentina Ulivi,<sup>5</sup> Marco Poggi,<sup>2</sup> Renato Zanatta,<sup>6</sup> Maddalena Iannaccone<sup>5</sup>

**To cite:** Campolo M, Oricco S, Cavicchio P, *et al.* Echocardiographic evaluation of four giant Aldabra tortoises (*Aldabrachelys gigantea*). *Veterinary Record Open* 2019;**6**:e000274. doi:10.1136/vetreco-2018-000274

Received 14 January 2018  
Revised 15 January 2019  
Accepted 20 August 2019

## ABSTRACT

**Objectives** In recent years echocardiography has become a good diagnostic tool in Zoo Medicine but in some cases, it is still a challenge. In Aldabra giant tortoise (*Aldabrachelys gigantea*) the big size of animals and the few individuals hosted in Zoo are critical points for the application of this diagnostic technique.

The purposes of this research were: to evaluate the feasibility of the diagnostic imaging technique on big-sized turtles; to define the echographic parameters for this species; and to describe the morphofunctional and physiological echographic characteristics of their cardiovascular system.

**Design** Repeated measures in vivo.

**Setting** Ultrasonography systematic description and Doppler analysis of the cardiovascular system of Aldabra giant tortoise were carried out; B-mode examination allowed the evaluation of the kinetics of the ventricle, the atria and the atrioventricular valves.

**Participants** 4 Aldabra giant tortoises (two adult males and two young females) hosted in two zoological gardens.

**Interventions** Echocardiography was performed placing the animals in ventral on a restraining platform raised from the floor, to provide adequate accessibility to the thoracic windows where the probe was placed. No chemical restraint was used.

**Primary and secondary outcome measures** Heart rate, systolic and diastolic areas and volumes, vessel diameters and blood flow velocity were measured.

**Results** Heart rate was  $21 \pm 4$  bpm (range 14–25 bpm). The averages of the diastolic and systolic area indexes linked to the subject weight were:  $21 \pm 3$  cm<sup>2</sup> and  $9 \pm 1$  cm<sup>2</sup>. The aortic annulus diameter in female specimens measured  $11.2 \pm 0.8$  mm, while it measured  $21.5 \pm 0.3$  mm in male species.

**Conclusion** Results confirm the effectiveness of echocardiography as a means to study and evaluate the cardiovascular system of this species even if more studies on a bigger number of patients would be necessary to develop the echocardiography technique.

## INTRODUCTION

The Indian Ocean islands were once home to an estimated 17 species of giant tortoises. By the beginning of the 19th century only one remained, the Aldabra giant tortoise *Geochelone gigantea*<sup>1</sup> listed on CITES Appendix II.<sup>2</sup> The reasons for extinction were principally

man's exploitation for food and the depredation of introduced species.<sup>3</sup> Despite legislation banning the killing or capturing of the tortoises by the early 1800s, the only substantial herds of wild Indian Ocean giant tortoises were to be found on the Aldabra Atoll in the southern Seychelles. To preserve this species and its natural habitat, in 1982, Aldabra was inscribed in the UNESCO World Heritage Sites.<sup>1</sup> The subgenus *Aldabrachelys* consists of seven species, all of which are referable to *G gigantea*,<sup>4</sup> classified as vulnerable in the International Union for Conservation of Nature Red List of Threatened Species.<sup>5</sup> During the last decades, significant initiatives have been created to support and promote freshwater turtle and tortoise conservation and long-term survival. To establish both in-range and out-of-range ex situ assurance colonies, initiation of captive breeding and management programmes through zoo and private breeding programmes have been developed.<sup>6</sup> Attempts to investigate the causes of illness and death among Aldabra giant tortoises, held in zoological collections, have been held back by lack of normal baseline physiological values for the species.<sup>7</sup> Echocardiography can be an effective diagnostic means in the medicine of zoo and wild animals, but to use this diagnostic technique in order to evaluate the state of health of certain animals, it is important first to define the ultrasound values and the physiological parameters of each individual species creating a database for further studies on ultrasound and evaluation of animal health. Complete chelonian semiotic data collection is not possible since the carapace reduces the chance to fully evaluate the coelomic organs and the diagnosis based on a clinical examination is usually poor.<sup>8</sup> In non-crocodilian reptiles, the circulation system is characterised by a peculiar large chamber called sinus venosus which receives blood from two precaval veins (right and left), a postcaval vein and from the left hepatic vein. It canalises



© British Veterinary Association 2019. Re-use permitted under CC BY-NC. No commercial re-use. Published by BMJ.

<sup>1</sup>Centro Veterinario Einaudi, Bari, Italy

<sup>2</sup>Centro Veterinario Imperiese, Imperia, Italy

<sup>3</sup>Giardino Zoologico città di Pistoia, Pistoia, Italy

<sup>4</sup>Zoom Torino, Torino, Italy

<sup>5</sup>Il Mondo degli Animali Esotici, Genova, Italy

<sup>6</sup>Veterinary Science, University of Turin, Torino, Italy

## Correspondence to

Dr Maddalena Iannaccone; veterinariaesotici@gmail.com



**Figure 1** Scheme of chambers and cardiac septa in turtles.

the deoxygenated blood from the systemic circulation to the right atrium. A series of muscular ridges divide the ventricle into three chambers, namely cavum pulmonale, arteriosum and venosum; these muscular ridges, associated with the timing of the ventricular contractions, provide for functional division in providing a separation of the well-oxygenated blood from the poorly oxygenated. From the cavum venosum originate the left and the right aortic arches in the cranial-ventral part, whereas from the cavum pulmonale, separated by the other two cava by an incomplete muscular septum called muscular ridge, the blood flows through the pulmonary ostium into the pulmonary artery<sup>9</sup> (figure 1). The absence of a clear intraventricular division makes unavoidable the presence of a shunt.

The atrioventricular valves are composed of a single cusp, their function is to prevent blood regurgitation from the ventricle into the atria during ventricular systole.

Coelomic ultrasonography scans have been carried out in different reptile species to evaluate the normal echo anatomy,<sup>8–12</sup> to study the reproductive physiology<sup>13,14</sup> and, in one case, as a diagnostic tool to identify pericardial effusion in a spur-thighed tortoise (*Testudo graeca*).<sup>15</sup> Doppler ultrasonography has been used to provide systematic descriptions of the cardiovascular system of loggerhead sea turtles (*Caretta caretta*),<sup>16</sup> red-eared terrapins (*Trachemys scripta elegans*),<sup>17</sup> Herman's tortoise (*Testudo hermanni*) and Russian tortoise (*Agryonemys horsfieldii*).<sup>18</sup> The aims of this

research were to evaluate the feasibility of the diagnostic imaging technique for heart evaluation on big-sized turtles; to define the normal echographic parameters; and to describe the morphofunctional and physiological characteristics of their cardiovascular system in the Aldabra giant tortoise, species of high conservation value,<sup>5</sup> but still unstudied in terms of echocardiography.

## MATERIALS AND METHODS

Four healthy Aldabra giant tortoises, housed at the Pistoia Zoological Garden (tortoise 1 and tortoise 4) and at the Zoom Zoological Park of Torino (tortoise 2 and tortoise 3), were included in this study (table 1). The tortoises were fed a diet of wild herbs, leafy vegetables and seasonal fruits, and supplemented two times a week with reptile multivitamin powder. Both Pistoia and Zoom Torino Zoos raised turtles in large indoor during winter times and outdoor exhibits in summer.

The tortoises were placed in ventral recumbency on a restraining platform raised from the floor, to provide adequate accessibility to the thoracic windows where the probe was placed. No chemical restraint was used and each ultrasonographic session lasted approximately 30 minutes. Animals were trained to this procedure with operant conditioning techniques using positive reinforcement as food rewards and tactile stimulation as this procedure has been shown to be less stressful for both animals and handlers and it also does not require chemical restraint of the tortoises.<sup>19</sup>

All the exams were made by only one operator. It was not possible to obtain the ECG evaluation during the ultrasonographic examination since animals were not anaesthetised and they could slightly move their back limbs causing artefacts. Examinations were carried out by using a portable Esaote MyLab30 ultrasound (Esaote, Genova, Italy) with a 3.5–5 MHz phased array probe. Subjects were positioned on the restraining platform, then the transducer was lubricated with ultrasound gel (GIMA, Gessate, Milano, Italy) and placed against the skin. To study kinetics, volumes and structure of the heart, right cervical acoustic window was used. The probe was placed with the marker oriented medially and a ventromedial inclination was used to optimise the image of the heart and visualise all the three chambers (*basal 1 view*). Clockwise rotation of the probe during the echocardiographic examination allowed switching

**Table 1** Animal data

| Animals |            |     |                      |             |                           |
|---------|------------|-----|----------------------|-------------|---------------------------|
| No      | House name | Sex | Estimate age (years) | Weight (kg) | Provenience               |
| 1       | Norberto   | M   | 90                   | 195         | Pistoia Zoological Garden |
| 2       | Ursus      | M   | 75                   | 155         | Zoom Torino               |
| 3       | Cassandra  | F   | 30                   | 75          | Zoom Torino               |
| 4       | Clara      | F   | 25                   | 70          | Pistoia Zoological Garden |

from a longitudinal projection parallel to the blood inflow tract, to a second longitudinal transverse projection to optimise the outflow tract (*basal 2 view*). Pulsed wave Doppler examination was carried out for the atrioventricular diastolic flow examination (basal 1 view) and the aortic and pulmonary flows (basal 2 view). Cine-loop and images were acquired during each scan and subsequently processed offline performing three measurements for each of the single parameters evaluated in all subjects. Various measurements were performed to determine ventricle size: end-diastolic and end-systolic lengths, areas and volumes. Diastolic and systolic volumes were calculated using the Area-Length (A-L) and the monoplane Simpson's (Simp) methods.<sup>19</sup> Values have been indexed to the subject's weight (Area/Weight \* 100, Volume/Weight \* 100). To evaluate the ventricular function, fractional area change (FAC) and ejection fraction (EF) were used. FAC resulted dividing the difference between end-diastolic area (EDA) and end-systolic area (ESA) by EDA and reporting to percentage (FAC:  $((EDA-ESA)/EDA) * 100$ ). EF was calculated through end-diastolic volume (EDV) and end-systolic volume (ESV) calculated with A-L ( $EF_{A-L}$ ) or monoplane Simpson's ( $EF_{SIMP}$ ) methods (EF:  $((EDV-ESV)/EDV) * 100$ ). The atrioventricular diastolic flow was analysed with the pulsed wave Doppler and Doppler colour flow examinations and velocity peaks were measured. Systolic flows through the aorta and the pulmonary artery were analysed by measuring the velocity peak (V) and velocity time integral (VTI) by pulsed wave Doppler. Heart rate was obtained by measuring the time between the beginnings of each pulsating flow. The aortic annulus was considered as the distance between two endocardial margins.

## RESULTS

B-mode echocardiography in the basal 1 view allowed to visualise the right atrium, the ventricle, the atrioventricular valves, the aorta and the left atrium (figure 2).

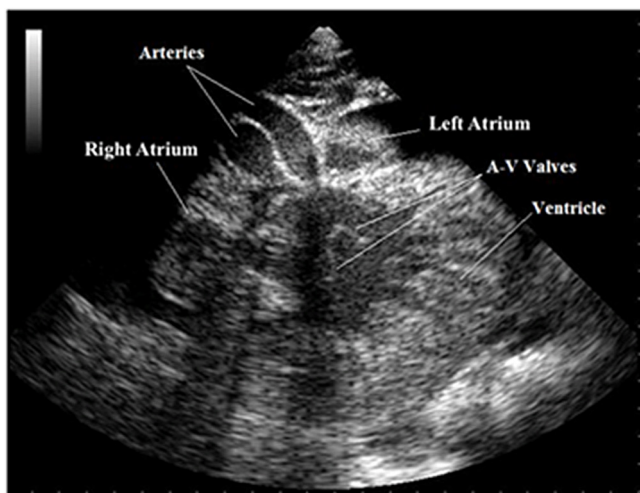


**Figure 2** Visualisation of the heart of *Aldabrachelys gigantea* in the basal 1 view.

The left atrium was best viewed using the left acoustic window. The circular shape of the ventricle, with a pointed part at the apex, was visible ultrasonographically, although it was not possible to distinguish the venosum, the arteriosum or the pulmonale cava within the ventricle. The endocardium appeared to be jagged and made up of a trabecular meshwork; in some tortoises it was possible to view the muscular ridge on which the atrioventricular cusps lean during the diastole by slightly tilting the probe. The atrial walls were proportionally thicker than in mammals, but thinner than the wall of the ventricle; during the ultrasound it is evident how they move with a major systolic-diastolic range participating actively to the ventricular diastole. The atrioventricular valves have a single concave spoon-shaped cusp that implants medially on the base of the interatrial septum. The opening movement of those valves has a single range during the whole diastolic phase differing from mammals where the valves close slightly after the rapid filling phase and then reopen after the atrial contraction.<sup>20</sup> Heart rate was  $21 \pm 4$  bpm (range 14–25 bpm). Of the four tortoises, two out of four (tortoise 1 and tortoise 2) had trace to trivial amounts of hypoechoic pericardial effusion; of those with pericardial effusion, none demonstrated signs of cardiac tamponade. Areas ( $\text{cm}^2$ ) and volumes (ml) (table 2), obtained with two different methods (A-L and monoplane Simpson), are related to the weight (table 3). The averages of the diastolic and systolic area indexes linked to the subject weight were:  $21 \pm 3 \text{ cm}^2$  and  $9 \pm 1 \text{ cm}^2$ , whereas the averages of volumes measured respectively with the Area-Length and the monoplane Simpson's methods indexed to the subject weight were: diastolic A-L:  $61 \pm 4 \text{ ml}$ , diastolic Simp:  $59 \pm 3 \text{ ml}$ , systolic A-L:  $18 \pm 3 \text{ ml}$ , systolic Simp:  $17 \pm 3 \text{ ml}$ .

The indexes of ventricular performance are listed in table 3 and the averages of FAC,  $EF_{A-L}$  and  $EF_{SIMP}$  values were:  $55\% \pm 6\%$ ,  $70\% \pm 5\%$  and  $72\% \pm 5\%$ .

The aortic flow resulted to be monophasic and asymmetric, and the acceleration phase was shorter than the deceleration phase (figure 3). Pulmonary flow shows a steep acceleration phase reaching higher velocity compared with the aortic flow velocity (table 4); a long plateau phase follows this acceleration (figure 4). The atrioventricular flow is monophasic and bidirectional (figure 5): one flow from the left atrium into the cavum arteriosum and one flow from the right atrium into venosum-pulmonale cava. The aortic annulus diameter in female species measured  $11.2 \pm 0.8 \text{ mm}$ , while it measured  $21.5 \pm 0.3 \text{ mm}$  in male species (table 5). M-mode examination was not applicable. Quality of ultrasound examination decreases with heavier patients.

## DISCUSSION

This study demonstrates the efficacy of using ultrasound to evaluate morphology and heart function of Aldabra giant tortoise (*Aldabrachelys gigantea*). Doppler analysis and ultrasonography systematic description of the cardiovascular system were previously reported for loggerhead sea

**Table 2** Diastolic and systolic areas and volumes

|           | Weight (kg) | Diastolic area (cm <sup>2</sup> ) | Systolic area (cm <sup>2</sup> ) | Diastolic volume A-L (ml) | Systolic volume A-L (ml) | Diastolic volume Simp (ml) | Systolic volume Simp (ml) |
|-----------|-------------|-----------------------------------|----------------------------------|---------------------------|--------------------------|----------------------------|---------------------------|
| Norberto  | 195         | 33.8                              | 17.3                             | 117.8                     | 33.5                     | 105.7                      | 33.8                      |
| Ursus     | 155         | 30.1                              | 13.6                             | 117.6                     | 33.5                     | 89.7                       | 26.2                      |
| Cassandra | 75          | 17.3                              | 7.7                              | 44.8                      | 17.8                     | 46.5                       | 15.0                      |
| Clara     | 70          | 15.8                              | 5.9                              | 40.4                      | 10.4                     | 41.6                       | 9.3                       |

A-L, Area-Length method; Simp, Simpson's method.

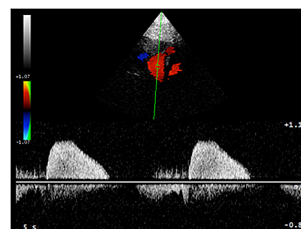
turtle (*C caretta*)<sup>16</sup> and red-eared slider terrapin (*T scripta elegans*).<sup>17</sup> Considering the anatomical differences among chelonian species and the influence of these differences on the echographic exam, it is important, at first, to define the physiological echographic parameters of any individual species in order to create a valid echographic method for evaluation of anatomical structures in chelonids.<sup>8</sup> The quality of the echocardiographic procedure is closely associated to the cooperation of the patient. The difficulties arising from an uncooperative patient are expressed in a sonographic reverberation of waves back, with a misinterpretation of the signal. This is why we should always perform the procedure on animals previously trained. Operant conditioning techniques using positive reinforcement were already reported as a valid method for husbandry training of giant tortoises.<sup>19</sup> B-mode examination allowed the evaluation of the kinetics of the ventricle, the two atria and the atrioventricular valves of the heart of four *A gigantea*. M-mode examination commonly used to study mammals' cardiac chamber sides and wall thicknesses, wall motion, great vessel dimensions and valve motion<sup>20</sup> is not applicable to Aldabra giant tortoises since the parasternal short-axis view would require a lateral approach prevented by the carapace. Areas and volumes appear to be highly connected to the weight. According to the guidelines of the American Society of Echocardiography,<sup>21</sup> the monoplane Simpson's method and the A-L method were used to calculate volumes. The geometry of the ventricle differs from the ellipsoid, the geometric figure on which the A-L method is based, so the Simpson's method could be more effective and widespread than the other one, but it is necessary to analyse a greater number of patients to be able to statistically evaluate and confirm this hypothesis. The aortic annulus was observed to be in proportion with the size of the animal and the valve diameter measurement showed

a wide range (10.2–22.0 mm) (table 5). Tortoises 3 and 4 result to have an aortic annulus diameter of 11.2±0.8 mm, while the large-sized males have an aortic annulus diameter of 21.5±0.3 mm. Doppler examination of the ventricular outflow indicates a clear difference between the pulmonary and the aortic flow, both in speed and morphology; this can be due to the differences between pulmonary and systemic pressures and to the presence of a single ventricle. Under physiological condition, pulmonary arterial diastolic pressure is lower than systemic diastolic pressure; this allows during early systole a precocious opening of the pulmonary valve with a flow directed exclusively into the pulmonary artery reaching a velocity of 1.7–1.8 m/s (table 4). Shelton and Burggren described this phase in *Pseudemys* and *Testudo* with an experimental haemodynamic analysis reporting a 100 ms delay of the aortic flow compared with the pulmonary flow in patients with a heart rate of 23–30 bpm.<sup>22</sup> This delay in *A gigantea* is greater (about 150 ms) probably due to the lower heart rate (21±4 bpm). The aortic flow is more 'potbellied' (figure 3) and has V and VTI lower than the pulmonary flow (table 4), where the velocity is greater in the first part, and then decreases and stabilises with a plateau of the entire duration of the ventricular output (figure 4). The pulmonary flow lasts longer than the aortic flow, and the aortic stroke volume is 13 per cent lower than the pulmonary stroke volume according to Shelton and Burggren.<sup>22</sup> The pulmonary flow measurement might be underestimated due to a poor alignment with this same flow: the carapace restricts the probe movements and prevents to place the sample volume line parallel to the pulmonary artery flow that is more cranial-medium-ventral compared with the aortas. Blood reaches the sinus venosus through the systemic circulation with the left vena precava, the right vena precava, the vena hepatica and the vena postcava.<sup>16</sup> The sinus venosus characterised by walls thinner than the atrium receives the blood and forces it into the

**Table 3** FAC, EF<sub>A-L</sub> and EF<sub>SIMP</sub> values

|           | FAC (%) | EF <sub>A-L</sub> (%) | EF <sub>SIMP</sub> (%) |
|-----------|---------|-----------------------|------------------------|
| Norberto  | 49.0    | 70.0                  | 68.0                   |
| Ursus     | 55.0    | 71.0                  | 73.0                   |
| Cassandra | 55.0    | 70.0                  | 71.0                   |
| Clara     | 63.0    | 76.0                  | 78.0                   |

A-L, Area-Length method; EF, ejection fraction; FAC, fractional area change; SIMP, Simpson's method.

**Figure 3** Aortic flow 1.

**Table 4** Aortic (Ao) and pulmonary (Pulm) velocity (V) and velocity time integral (VTI) measured with the basal 2 view and atrioventricular (A-V) velocity (V) measured with the basal 1 view

|           | Ao V<br>(m/s) | Ao VTI<br>(cm) | Pulm V<br>(m/s) | Pulm VTI<br>(cm) | A-V V<br>(m/s) |
|-----------|---------------|----------------|-----------------|------------------|----------------|
| Norberto  | 0.76          | 59.7           | 1.66            | 155.3            | 0.8            |
| Ursus     | 0.84          | 65.7           | 1.70            | 167.3            | 1.0            |
| Cassandra | 0.80          | 63.3           | 1.72            | 127.0            | 0.9            |
| Clara     | 0.84          | 60.0           | 1.82            | 118.7            | 1.1            |

right atrium. During diastole the atrioventricular valve cusp opens, thus separating the venosus and arteriosum cava, blood flows into the ventricle, specifically in the cavum pulmonale passing through the cavum venosum. Simultaneously, the blood coming from the left and right pulmonary veins reaches the left atrium and, during diastole, fills the cavum arteriosum, isolated from the cavum venosum thanks to the opening of the atrioventricular cusps. During systole, the cavum pulmonale contracts overcoming the pulmonary resistance and facilitating the ejection into the pulmonary artery through the valve ostium and, when the intraventricular pressure reaches aortic diastolic pressure the cavum arteriosum pumps blood into the aortas through the cavum venosum, which is already partially contracted (figure 6A).

The differences in pressure, the atrioventricular valves and the muscular ridge isolating the cavum pulmonale create a functional separation between the two circulations. During the first part of the systole, called isovolumetric contraction, the pressure in the cava increases until the pressure inside the cavum pulmonale exceeds the pulmonary artery pressure; the pulmonary valve opens causing a progressive decrease of volume and pressure in the cavum pulmonale. The difference between pulmonary and systemic pressures creates a slight asynchrony between the pulmonary and the aortic outflows preventing the oxygenated blood from mixing with the non-oxygenated blood, although a share of physiological shunt is inevitable as both oxygenated and non-oxygenated blood pass into the cavum venosum, as described by Hicks.<sup>23-27</sup> During diastole the blood flows from the atria to the cavum pulmonale (passing through the cavum venosum) and the cavum arteriosum. Early systole is unavoidable that a small amount of blood flows from the cavum venosum and arteriosum to

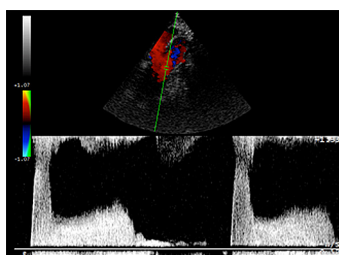


**Figure 4** Pulmonary flow 1.

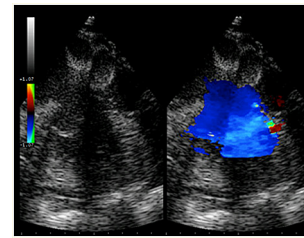


**Figure 5** Atrioventricular flow 1.

the cavum pulmonale and consequently up to the pulmonary artery, favouring a left to right shunt, thus a share of oxygenated blood is redirected into the pulmonary circulation. During diastole a residue of oxygenated blood in the cavum venosum passes in the cavum pulmonale (left to right shunt). A small share of blood that remains in the cavum venosum during the diastole favours a right to left shunt for the ejection of non-oxygenated blood into the systemic circulation, as described by Hicks.<sup>23</sup> This happens because when the cavum arteriosum contracts, it propels the muscular ridge ventrally, towards the cavum pulmonale, enabling the ejection into the aorta through cavum venosum, preventing the passage of blood in the cavum pulmonale.

When the pulmonary resistance increases substantially, a significant right to left shunt may occur as it happens during hibernation or apnoea for the aquatic species. This phenomenon is related to the increase of the pulmonary resistance that exceeds the systemic resistance and facilitates a complete blood passage in the systemic circulation (figure 6B).

Area and volume measurements were used to evaluate size and performance of the ventricular chamber. The aortic and pulmonary flows' different characteristics indicate a different pressure between the aortic and pulmonary circulation during diastole, which separates roughly oxygenated blood from non-oxygenated blood, significantly thus reducing the shunt. *A gigantea* is a terrestrial species that does not go into hibernation,<sup>28</sup> therefore the authors assume that no physiological reversal shunt, secondary to the pulmonary resistance increase, should occur. Any echocardiographic evidence of a reversal of the pulmonary and the aortic ejection timing, or any variation of the flows may result as an indicator of cardiac or respiratory pathological conditions. Future studies should focus on developing the echocardiography technique in order to develop a useful tool that will enable veterinarians to highlight the eventual

**Table 5** Aortic annulus measurement

|           | Ao annulus<br>(mm) |
|-----------|--------------------|
| Norberto  | 21.6               |
| Ursus     | 21.4               |
| Cassandra | 11.9               |
| Clara     | 10.5               |

Ao, aortic.

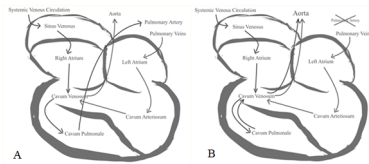


**Figure 6** (A) Blood flow directions in chelonian's heart. (B) Right to left shunt pattern.

presence of cardiac abnormalities and permitting early diagnosis in individuals of high biological and conservation value.

**Acknowledgements** The authors thank the Giardino Zoologico of Pistoia and the Zoom Torino for assenting this study, William Magnone, DVM, Richard M Bini, DVM, Domenico Iannaccone and Mariateresa Celebre for their technical support and assistance in carrying out the tests and the writing of the manuscript.

**Funding** The authors have not declared a specific grant for this research from any funding agency in the public, commercial or not-for-profit sectors.

**Competing interests** None declared.

**Provenance and peer review** Not commissioned; externally peer reviewed.

**Data availability statement** All data relevant to the study are included in the article.

**Open access** This is an open access article distributed in accordance with the Creative Commons Attribution Non Commercial (CC BY-NC 4.0) license, which permits others to distribute, remix, adapt, build upon this work non-commercially, and license their derivative works on different terms, provided the original work is properly cited, an indication of whether changes were made, and the use is non-commercial. See: <http://creativecommons.org/licenses/by-nc/4.0/>.

## REFERENCES

1. Spratt DMJ. Operation Curieuse: a conservation programme for the Aldabra giant tortoise *Geochelone gigantea* in the Republic of Seychelles. *Int Zoo Yearb* 1989;28:66–9.
2. Swingland IR, Klemens MW. *Geochelone gigantea*, Aldabran Giant Tortoise. In: *The conservation biology of tortoises*. Gland Switzerland: IUCN, 1989: Vol. 5. 105–8.
3. Stuart SN, Adams RJ. *Biodiversity in sub-Saharan Africa and its islands: conservation, management, and sustainable use*. Vol. 6. Gland, Switzerland: IUCN, 1990.
4. Frazier J. A neotype for the Aldabra tortoise, *Testudo gigantea* Schweigger, 1812. *Herpetol Rev* 2006;37:275–80.
5. Baillie J, Groombridge B. 1996 IUCN red list of threatened animals. Switzerland and Cambridge, UK IUCN, Gland; 1996.
6. Turtle Conservation Fund. A global action plan for conservation of tortoises and freshwater turtles. strategy and funding prospectus 2002-2007. Washington, DC Conservation International and Chelonian Research Foundation; 2002: 10–18.
7. Hart MG, Samour HJ, Spratt DMJ, *et al*. An analysis of haematological findings on a feral population of aldbabra giant tortoises (*Geochelone gigantea*). *Comparative Haematology International* 1991;1:145–9.
8. Valente AL, Parga ML, Espada Y, *et al*. Ultrasonographic imaging of loggerhead sea turtles (*Caretta caretta*). *Vet Rec* 2007;161:226–32.
9. Mader DR. Cardiopulmonary Anatomy and Physiology. In: *Reptile medicine and surgery*. WB Saunders CO, Philadelphia, 2006: 124–9.
10. Penninck DG, Stewart JS, Paul-Murphy J, *et al*. Ultrasonography of the California desert tortoise (*Xerobates agassizi*): anatomy and application. *Vet Radiol* 1991;32:112–6.
11. Holz RM, Holz P. Electrocardiography in anaesthetised red-eared sliders (*Trachemys scripta elegans*). *Res Vet Sci* 1995;58:67–9.
12. Redrobe S. An introduction to chelonian radiography and ultrasonography. *B.C.G. Testudo* 1997;4:34–41.
13. Martorell J, Espada Y, Ruiz de Gopegui R. Normal echoanatomy of the red-eared slider terrapin (*Trachemys scripta elegans*). *Vet Rec* 2004;155:417–20.
14. Robeck TR, Rostal DC, Burchfield PM, *et al*. Ultrasound imaging of reproductive organs and eggs in Galapagos tortoises, *Geochelone elephantopus* spp. *Zoo Biol* 1990;9:349–59.
15. Redrobe SP, Scudamore CL. Ultrasonographic diagnosis of pericardial effusion and atrial dilation in a spur-thighed tortoise (*Testudo graeca*). *Vet Rec* 2000;146:183–5.
16. Valente AL, Parga ML, Espada Y, *et al*. Evaluation of Doppler ultrasonography for the measurement of blood flow in young loggerhead sea turtles (*Caretta caretta*). *Vet J* 2008;176:385–92.
17. Poser H, Russello G, Zanella A, *et al*. Two-dimensional and Doppler echocardiographic findings in healthy non-sedated red-eared slider terrapins (*Trachemys scripta elegans*). *Vet Res Commun* 2011;35:511–20.
18. Prütz M, Hungerbühler S, Laß M, *et al*. Contrast echocardiography for analysis of heart anatomy in tortoises. *Tierarztl Praxis Ausg K Kleintiere Heimtiere* 2015;43:231–7.
19. Weiss E, Wilson S. The use of classical and operant conditioning in training Aldabra tortoises (*Geochelone gigantea*), for venipuncture and other, husbandry issues. *J Appl Anim Welf Sci* 2003;6:33–8.
20. Kittleson MD, Kienle RD. Normal clinical cardiovascular physiology. In: Kittleson MD, Kienle RD, eds. *Small animal cardiovascular medicine*. Mosby St. Louis, MO, 1998: 11–35.
21. Schiller NB, Shah PM, Crawford M, *et al*. Recommendations for quantitation of the left ventricle by two-dimensional echocardiography. *Journal of the American Society of Echocardiography* 1989;2:358–67.
22. Shelton G, Burggren W. Cardiovascular dynamics of the Chelonia during apnoea and lung ventilation. *J Exp Biol* 1976;64:323–43.
23. Hicks JW. Adrenergic and cholinergic regulation of intracardiac shunting. *Physiol Zool* 1994;67:1325–46.
24. Hicks J, Comeau S. Vagal Regulation of intracardiac shunting in the turtle *Pseudemys scripta*. *J Exp Biol* 1994;186:109–26.
25. Hicks JW, Ishimatsu A, Molloi S, *et al*. The mechanism of cardiac shunting in reptiles: a new synthesis. *J Exp Biol* 1996;199:1435–46.
26. Ishimatsu A, Hicks JW, Heisler N. Analysis of cardiac shunting in the turtle *Trachemys (Pseudemys) scripta*: application of the three outflow vessel model. *J Exp Biol* 1996;199:2667–77.
27. Wang T, Hicks JW. The interaction of pulmonary ventilation and the right-left shunt on arterial oxygen levels. *J Exp Biol* 1996;199:2121–9.
28. Boyer TH, Boyer DM. Turtles, tortoises and terrapins. In: Mader DR, ed. *Reptile medicine and surgery*. WB Saunders CO, Philadelphia, 2006: 78–98.